RERC 2014 Reno

Green to Orange Color-Tuneable Emission of $Tb_2Mo_3O_{12}:Sm^{3+}$

Florian Baur*, Saba Tadesse, and Thomas Jüstel*

Department of Chemical Engineering, Münster University of Applied Sciences, Stegerwaldstr. 39, 48565 Steinfurt, Germany
**Corresponding authors: florian.baur@fh-muenster.de, tj@fh-muenster.de*

Rare Earth Research Conference 2014, June 22-27, Squaw Valley, CA, USA

Introduction

For solid state lighting the most common approach is the combination of a blue emitting LED with a yellow emitting phosphor powder or ceramic. This combination yields high luminous efficiency (LE). However, its cool-white light is not generally suitable for interior lighting. To produce warm-white light a red emitting phosphor such as $CaAlSiN_3:Eu^{2+}$ and $Sr_2Si_5N_8:Eu^{2+}$ is thus added. The disadvantage of these phosphors it their broad emission band that extends to the NIR spectral region. This results in a lower LE than what is theoretically possible [1].

Red line emitters such as Eu^{3+}, Sm^{3+} and Pr^{3+} offer an emission spectrum that allows much higher LE. While Eu^{3+} has been widely investigated, Sm^{3+} is less deeply examined. This is mostly due to its low quantum effiency, which is related to cross relaxation processes. However, with broad absorption multiplets in the blue spectral region, mostly arising from transitions to the ^4I_j states, Sm^{3+} poses an interesting alternative as red converter for blue light-emitting diodes. To further increase absorption in the blue spectral range, a Tb^{3+} comprising host material was chosen. A very efficient energy transfer from Tb^{3+} to Sm^{3+} allows the emission color to be tuned from green to orange by varying the Tb^{3+}/Sm^{3+} ratio.

Material Properties

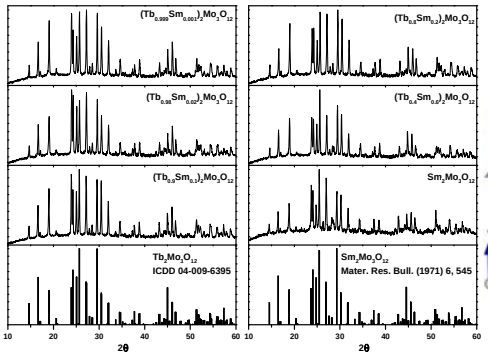

Fig. 1. XRD patterns of synthesized $(Tb_{1-x}Sm_x)_2Mo_3O_{12}$ powders and of $Tb_2Mo_3O_{12}$ and $Sm_2Mo_3O_{12}$ references (orthorhombic, *Pba*2).

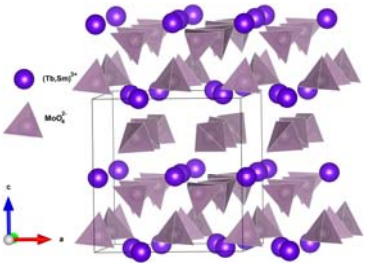

Fig. 2. Crystal structure of $(Tb_{1-x}Sm_x)_2Mo_3O_{12}$ [2,3].

Results and Discussion

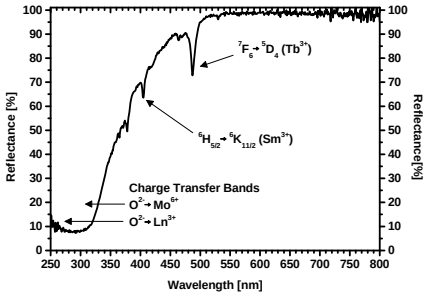

Fig. 3. Reflection spectrum of $(Tb_{0.98}Sm_{0.02})_2Mo_3O_{12}$ with prominent transitions marked.

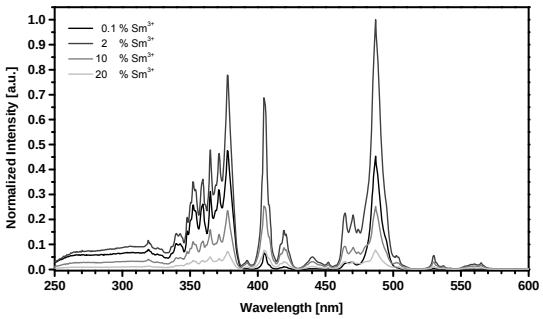

Fig. 4. Excitation spectra of $(Tb_{1-x}Sm_x)_2Mo_3O_{12}$ with different Sm^{3+} concentrations monitored at 648.5 nm (Sm^{3+} $^4G_{5/2} \rightarrow {}^6H_{9/2}$).

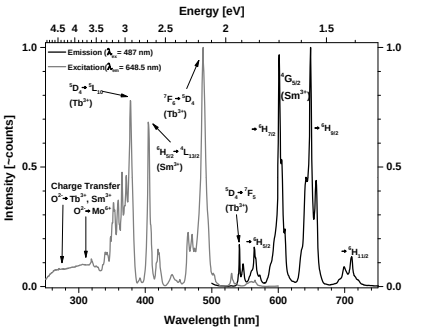

Fig. 5. Excitation and emission spectra of $(Tb_{0.98}Sm_{0.02})_2Mo_3O_{12}$ with transitions assigned to prominent lines.

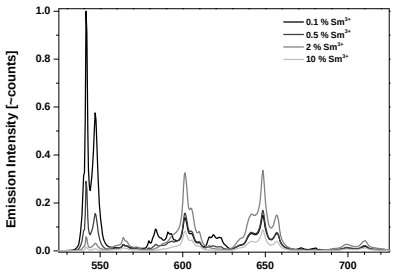

Fig. 6. Emission spectra of $(Tb_{1-x}Sm_x)_2Mo_3O_{12}$ upon 487 nm excitation.

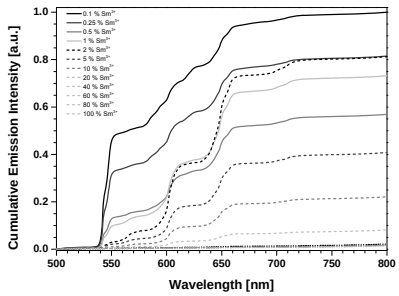

Fig. 7. Cumulative emission intensities of $(Tb_{1-x}Sm_x)_2Mo_3O_{12}$ upon 487 nm excitation.

Fig. 3 depicts the reflection spectrum of the 2% Sm^{3+} sample. The broad absorption band in the UV range is a host related absorption process caused by charge transfer from O^{2-} ligands to Mo^{6+} and Tb^{3+}/Sm^{3+} atoms, respectively. Additional absorption lines are easily discernible which arise from intraconfigurational $[Xe]4f^n \rightarrow [Xe]4f^n$ transitions of both Tb^{3+} and Sm^{3+}. The strong reflectance in the long wavelength range indicates the high quality of the synthesized powders. Excitation spectra recorded by monitoring Sm^{3+} 648.5 nm emission are presented in Fig. 4. The prominent Tb^{3+} excitation line multiplet around 487 nm shows the existence of energy transfer from Tb^{3+} to Sm^{3+}.

At Sm^{3+} concentrations below 10% both orange Sm^{3+} and green Tb^{3+} emission can be observed as depicted in Fig. 6. The $^5D_4 \rightarrow {}^7F_5$ emission of Tb^{3+} decreases with increasing Sm^{3+} concentration due to increased energy transfer efficiency. The Sm^{3+} emission increases with Sm^{3+} concentration until a maximum is reached at 2 %. At higher concentrations the intensity decreases due to concentration quenching of Sm^{3+}. Fig. 7 depicts the cummulative emission intensities. The highest intensity is achieved with the 0.1 % Sm^{3+} sample. This is a direct consequence of the low quantum efficiency of Sm^{3+} as the energy received from Tb^{3+} is not completely converted to photons. CIE1931 color points were calculated and are presented in Fig. 8.

To further investigate the nature of the $Tb^{3+} \rightarrow Sm^{3+}$ energy transfer, decay curves were recorded (Fig. 9). At low Sm^{3+} concentrations the 648.5 nm emission increases for approx. 0.5 ms after the 487 nm excitation source was switched off. This is the so-called rise time, i.e. the period of time in which the fraction of Sm^{3+} ions that receive energy from Tb^{3+} ions is larger than the number of Sm^{3+} ions emitting a photon. Rise-times are characteristic of sensitized emission. However, rise-times in the ms range are rarely observed. The curves were fitted to determine the half-times τ_1 and τ_2 of the energy transfer and the Sm^{3+} excited state, respectively. τ_1 decreases with increasing Sm^{3+} concentration. This is to be expected as the mean distance between Tb^{3+} and Sm^{3+} decreases.

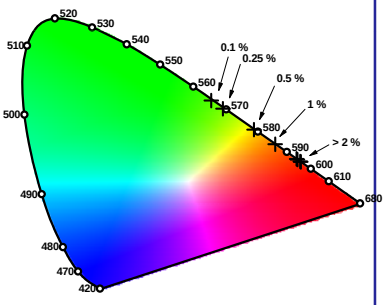

Fig. 7. CIE1931 color points of $(Tb_{1-x}Sm_x)_2Mo_3O_{12}$.

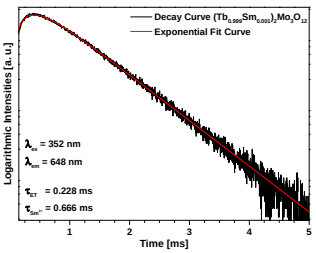

Fig. 9. Emission spectra of Eu^{3+} $^5D_0 \rightarrow {}^7F_2$ recorded at temperatures from 100 to 500 K under 487 nm excitation.

This work was generously supported by Merck KGaA, Darmstadt, Germany.
References: [1] Zukauskas et al., Appl. Phys. Lett. 93 (2008) 51115,
[2] ICDD 04-009-6395, [3] Momma and Izumi, J. Appl. Crystallogr. 44 (2011) 1272